Ignition of CH_4 by Counterflowing Hot Air Diluted with Combustion Products

Keum Mi Song* and Chang Bo Oh*
cboh@pknu.ac.kr
* Department of Safety Engineering, Pukyoung National University, South Korea.

Abstract
Ignition temperature of CH_4 by counterflowing hot air diluted with combustion products was investigated numerically using a flame-controlling continuation. GRI-v3.0 was used for the calculation of chemical reaction rates in all the computations. The maximum H radical concentrations were presented in the function of the global strain rate, and showed S-curve behavior. Ignition temperature of CH_4 was determined using S-curve of the H radical concentration. The effects of strain rate on the ignition temperature of CH_4 were investigated with the dilution rate (Ω) of combustion products. Pollutant emission characteristics and flame structures were investigated with a steady counterflow flame code, OPPDIF. The emission indices for major pollutant were introduced to compare the pollutant emission quantitatively. EINOx for the condition considered in this study ($\Omega \leq 0.5$) was still higher than that of usual low-temperature air nonpremixed combustion.

Introduction
The global warming and environmental pollution problems arise from the combustion systems that utilize the fossil fuels becomes more serious recently. Combustion process of the fossil fuels essentially emits green-house gases and pollutant, such as NOx, SOx, and soot. Thus, every effort to reduce such green-house gas and pollutants is progressing all over the world. The best way to reduce the main green-house gas, CO_2, emitted during the combustion of fossil fuels is to enhance the combustion efficiency. High-temperature air combustion is a promising technique to improve the combustion efficiency as well as to reduce the pollutant emission. High-temperature air combustion improves the combustion efficiency by recycling exhaust heat to the supplying air stream [1, 2]. In addition, it was known that flameless combustion with small temperature gradient in all direction can be achieved by making the supplying air stream be high-temperature and low-oxygen content oxidizer. This flameless combustion can be possible when the temperature of supplying air steam is over the auto-ignition temperature of fuel. The oxygen concentration in air stream is closely related with the pollutant emission from the flameless combustion.

It has been known that there are three combustion regions in the high-temperature air combustion in the respect of mixing of fuel and air [1]. The first one is BF/BA region where the combustion reactions occur between diluted fuel with burnt gases (BF) and diluted air with burnt gases (BA). Reactions between diluted fuel with burnt gases and fresh air (A) occur at the second region (BF/A), and combustion between fresh fuel (F) and diluted air with burnt gases at the third region (F/BA). Previous fundamental studies regarding the high-temperature air combustion have mainly focused on the BF/A region [3,4]. It is necessary to investigate the combustion characteristics in the other regions, such as F/BA and BF/BA, to understand the high-temperature air combustion in more detail.

Thus, the main objective of this paper is to investigate the auto-ignition temperature of CH_4 by counterflowing hot air diluted with combustion products for considering the high-

temperature air combustion characteristics in F/BA region. In addition, flame structure and pollutant emission characteristics of the F/BA combustion region were investigated.

Numerical Procedure

An OPPDIF code [5] usually used for the simulation of steady counterflow flame is not applicable for the investigation of ignition since which is unsteady phenomenon essentially. In this study, a flame-controlling continuation method (FCCM) developed by Nishioka et al. [6] was used to obtain an ignition temperature of couterflowing CH_4 by hot air mixed with combustion products. The maximum H concentration was presented in the function of the inverse global strain rate, and showed S-curve behavior related with the extinction and ignition. The numerical algorithm of FCCM is very similar to that of OPPDIF except boundary conditions and dependent variables. The detailed numerical procedure of FCCM was described elsewhere [6]. The OPPDIF code was used for steady counterflow flame structure and pollutant emission characteristics. Steady OPPDIF results were used as initial conditions for the computation with FCCM.

In this study, we focus on the ignition and emission characteristics of F/BA region among the highly-preheated air combustion regions. Thus, the air stream was mixed with the combustion products and its temperature was raised sufficiently such that inflowing fuel was ignited. The concentration of the combustion products was computed using UPSR (Unsteady Perfectly-Stirred Reactor) code [7]. The UPSR code computed the temperature and species concentration for the condition where fuel and air are perfectly mixed. First, the concentrations of main combustion products of CH_4 were evaluated for a condition of the equivalence ratio (Φ) of 1.0 using UPSR. All species concentrations formed from the pyrolysis of the main combustion products and air at supplying high-temperature air stream were also computed with UPSR. The concentrations of all the species were used as the inflow boundary condition when steady flame structure was computed using OPPDIF code.

Numerical Conditions

In order to investigate the ignition characteristics of fuel, flow field that consisted of counterflowing CH_4 and hot air streams was used as a geometry in this study. The separation distance (L) between fuel and air nozzles was 15 mm. For chemical reactions GRI-v3.0, which considers 53 species and 325 reactions, was used for all computations. The radiation effects were not considered in this study.

The temperature of fuel stream was fixed to 300 K, and the temperature of air stream mixed with the combustion products was varied from lower value to sufficiently-higher one. The pressure was fixed to 1 atm for all conditions. The volume fraction of O_2 and N_2 was 21% and 79%, respectively, for pure air stream. In case that the combustion products were mixed with pure air, concentrations of the combustion products were varied to the dilution rate (Ω). The dilution rate was defined as follows:

$$\Omega = \frac{volume\ of\ product\ gases}{volume\ of\ total\ gases\ in\ air\ steam} \tag{1}$$

A global strain rate (a_g) [8], which is important parameter to characterize diffusion flames, was introduced in this study.

$$a_g = \frac{2V_a}{L}\left(1 + \frac{V_f\sqrt{\rho_f}}{V_a\sqrt{\rho_a}}\right) \tag{2}$$

where, V_f and V_a is separately velocity of fuel and oxidizer, and ρ_f and ρ_a is separately density of fuel and oxidizer.

In order to quantify the emission characteristics of pollutants, emission indices [9, 10] for CO, CO_2, NO and NO_2 were evaluated using the following equation (3):

$$EI_i = \frac{\int_0^L W_i \dot{\omega}_i dx}{-\int_0^L W_{CH_4} \dot{\omega}_{CH_4} dx} \tag{3}$$

where, i is the species CO, CO_2, NO and NO_2; W_i is the molecular weight of species i; $\dot{\omega}_i$ is the molar production rate of species i; L is the separation distance between fuel and oxidizer nozzles.

Results and Discussion

It was known that the maximum H radical concentration versus strain rate provides more precise ignition temperature data than the maximum temperature [6, 11]. In this study, thus, we adopted the maximum H radical variation for the investigation of ignition temperature. Fig. 1 shows the maximum H radical concentration versus the inverse of the global strain rate for case of pure air stream. For investigation of ignition characteristics, the temperature of inflowing air stream (T_O) was varied from 700 K to 1270 K. The variation of the H radical shows a typical S-curve behavior that is directly related with the extinction and ignition characteristics of nonpremixed flame of CH_4-pure air. The first turning points located at higher concentration of H radical are extinction points for each inflowing condition, and the second turning points located at lower concentration are ignition points. For T_O = 700 K and 900 K, the ignition points were not identified for considered strain rate range. This means that the fuel cannot be ignited for the strain rate range considered. At $T_O \geq 1100$ K, the shapes of second turning points were not monotonous but two-stage behavior although the second turning points existed apparently. For case of two-stage-ignition, I_1 and I_2 were known as primary and secondary ignition points, respectively.

Fig. 2 shows the maximum H radical response to the global strain rate when the combustion products are mixed in the air stream. The dilution rate, Ω, was varied to 0 (pure air) to 0.5. At $\Omega \geq 0.4$, the second turning point was not observed. In previous studies [12-16], the upper secondary ignition point (I_2) was rounded apparently. However, there were cases that the first ignition turning point was not observed clearly when the combustion products were mixed in the air stream as shown in Fig. 2. Thus, the secondary ignition point was selected as an ignition point in this study. The ignition temperature was defined by the temperature of air stream at the nozzle exit boundary. The difference in the global strain rates at the two ignition turning points, I_1 and I_2, was not so large because the horizontal axis represents the log scale value of the global strain rate.

Fig. 3 shows the ignition temperature of CH_4 versus the global strain rate. The ignition temperature increases with the global strain rate for a fixed dilution rate. Furthermore, the ignition temperature increases with the dilution rate for a fixed global strain rate. For large global strain rates, the increase rate of the ignition temperature further increases compared to the increase rate of dilution rate. As expected, these results mean that the ignition temperature increases as the dilution rate of combustion products becomes larger. It can be identified that the ignition of CH_4 is much more difficult as both the global strain rate and the dilution rate increase. For clarity, those ignition temperatures and trend obtained in this study will be validated using the experimental results in near future.

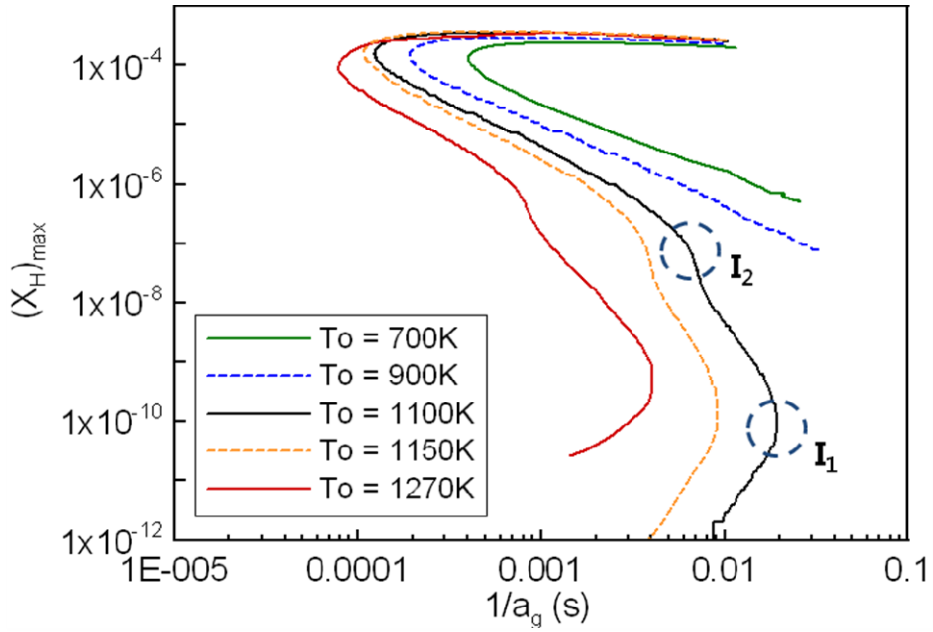

Figure 1. Response of the maximum H mole fraction to the global strain rate for pure air stream condition.

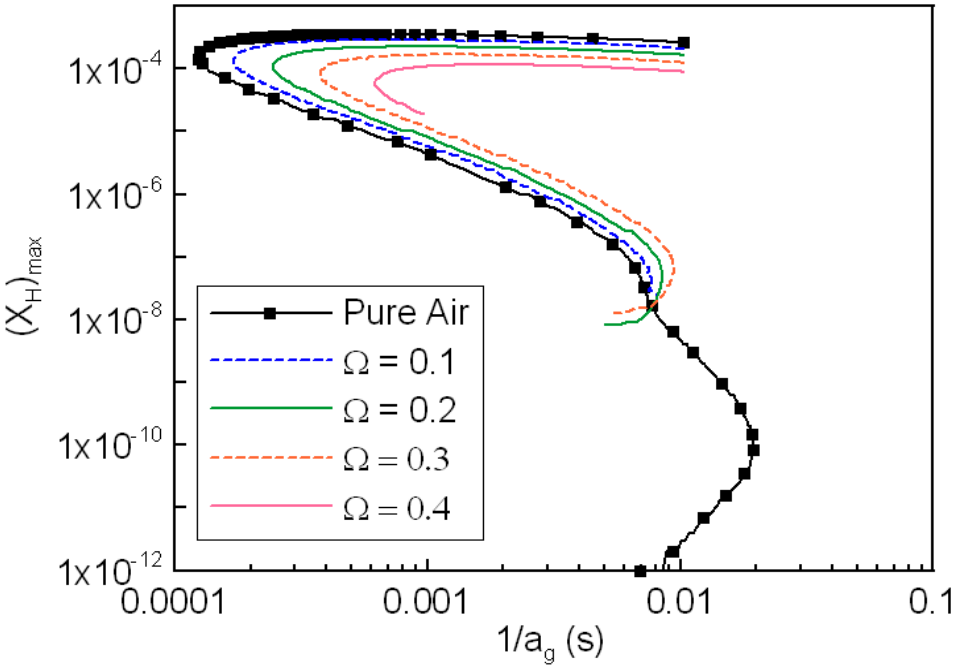

Figure 2. Response of the maximum H mole fraction to the global strain rate for case that the combustion products are mixed in the air stream at T_O=1100 K.

Figs 4 through 8 show the flame structure and pollutant emission characteristics of CH_4 nonpremixed flame ignited by hot air mixed with combustion products. Fig. 4 shows the distributions of the temperature and axial velocity with the variation of the dilution rate at a_g = 1000 (1/s). The air stream temperature was determined to be over 10 K than the ignition temperature for given global strain rate and dilution rate shown in Fig. 3. The volumetric percentage of oxygen in the air stream was 21% for pure air and 10.5% at Ω = 0.5, respectively (Table 1). The peak flame temperature decreases and the difference between the

peak and supplying air stream temperatures decreases as the dilution rate becomes larger. The peak flame temperature of Ω = 0.5 was about 2000 K. Those peak flame temperatures and differences between the peak and supplying air stream temperatures for various dilution rate are still higher compared to that of typical high-temperature air combustion. The results of Fig. 4 imply that proper high-temperature air combustion in F/BA region cannot be observed at Ω ≤ 0.5.

Figs. 5 and 6 show the distributions of NO and CO mole fraction for the same condition to that of Fig. 4. The concentrations of those two species were much reduced with increasing the dilution rate. Especially NO for pure air was remarkably reduced to 1/8 compared to the case of Ω = 0.5. Simultaneous increment in the supplying temperature of air stream and the dilution rate of combustion products are still effective for the NO and CO reduction in F/BA region. However, as shown in Fig. 4, the peak temperature and differences between the peak and supplying air stream temperatures are still high, thus, we needs to increase the dilution rate of combustion products in the air stream for the further reduction of the pollutants.

Table 1. Composition of the main species in the air stream with the variation of dilution rate.

species	Ω=0.1	Ω=0.2	Ω=0.3	Ω=0.4	Ω=0.5
O2	0.189	0.168	0.147	0.126	0.105
N2	0.782	0.774	0.766	0.758	0.750
CO	0.001	0.002	0.003	0.004	0.005
CO2	0.009	0.018	0.027	0.036	0.045
H2O	0.019	0.038	0.057	0.076	0.095

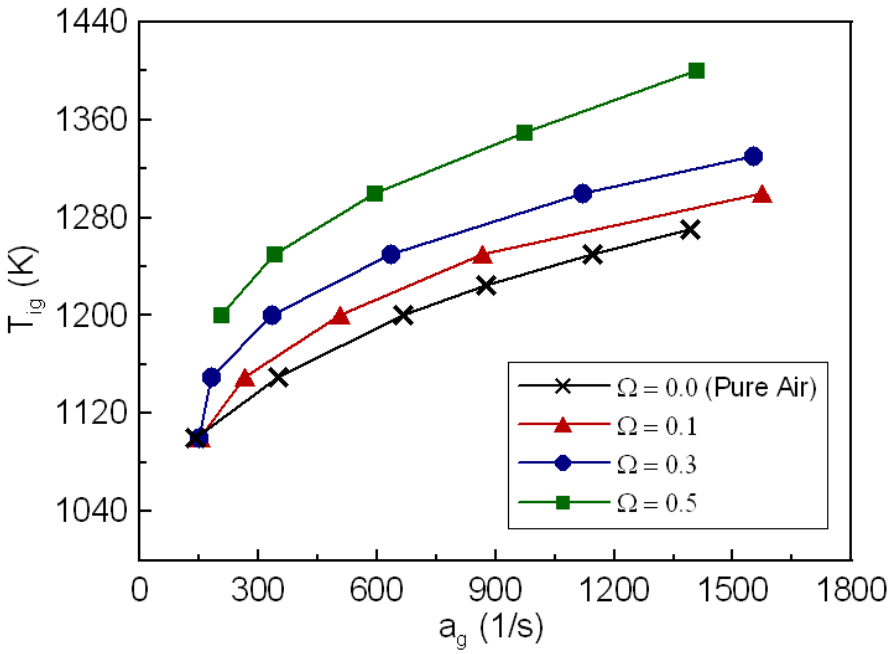

Figure 3. Ignition temperature of CH_4 versus the global strain rate.

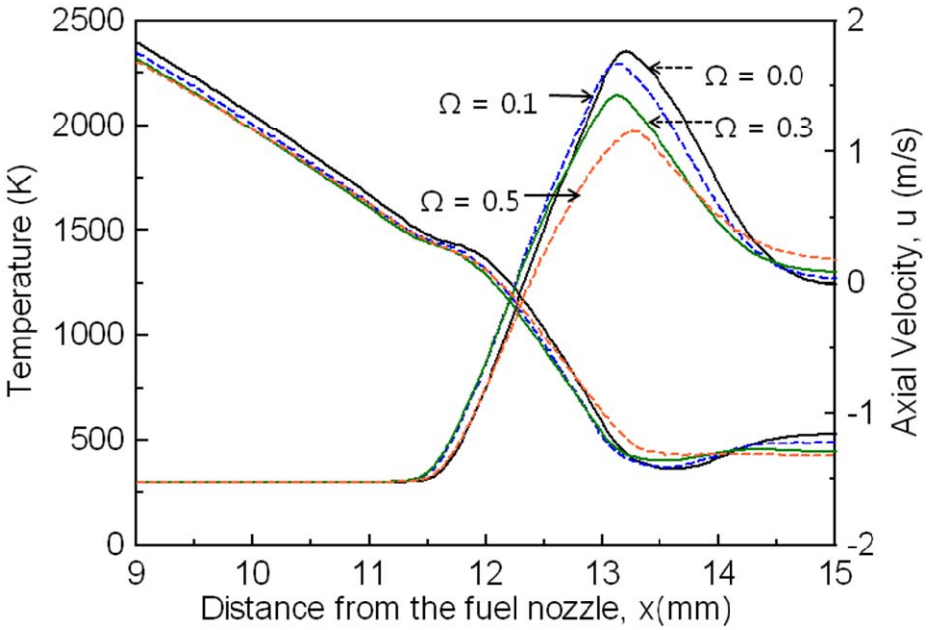

Figure 4. Distributions of the temperature and axial velocity of CH_4 nonpremixed flame ignited by hot air with the variation or dilution rate at a_g=1000 (1/s).

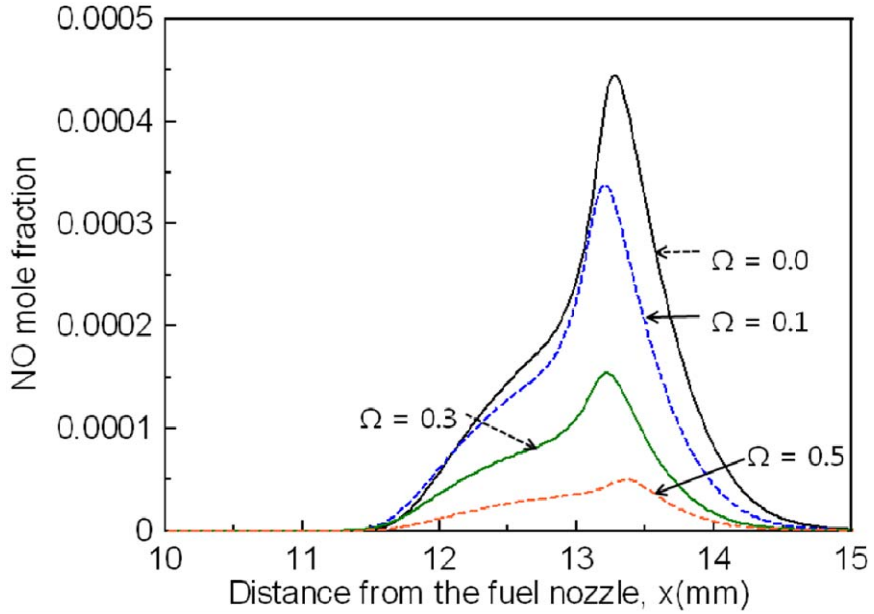

Figure 5. Distribution of NO mole fraction CH_4 nonpremixed flame ignited by hot air with the variation or dilution rate at a_g=1000 (1/s).

In order to compare the pollutant emission quantitatively, emission indices for NO, NO_2, CO and CO_2 were presented in Figs. 7 and 8. EINO decreased remarkably but $EINO_2$ increased gradually with increasing the dilution rate for the fixed global strain rate. Consequently, total EINOx (EINO + $EINO_2$) decreased with increasing the dilution rate since $EINO_2$ was very small compared to the EINO. It should be noted that, however, the EINO at $\Omega \leq 0.5$ in F/BA region was still higher than that of usual low-temperature air nonpremixed flame [10] or BF/A region [3]. In Fig. 8, EICO decreased slightly and $EICO_2$ increased gradually with increasing the dilution rate. This result implies that the BF/A region of high-

temperature air combustor is still effective in reducing the CO emission by increasing the dilution rate but is not effective in reducing the CO_2 emission even though the dilution rate increases.

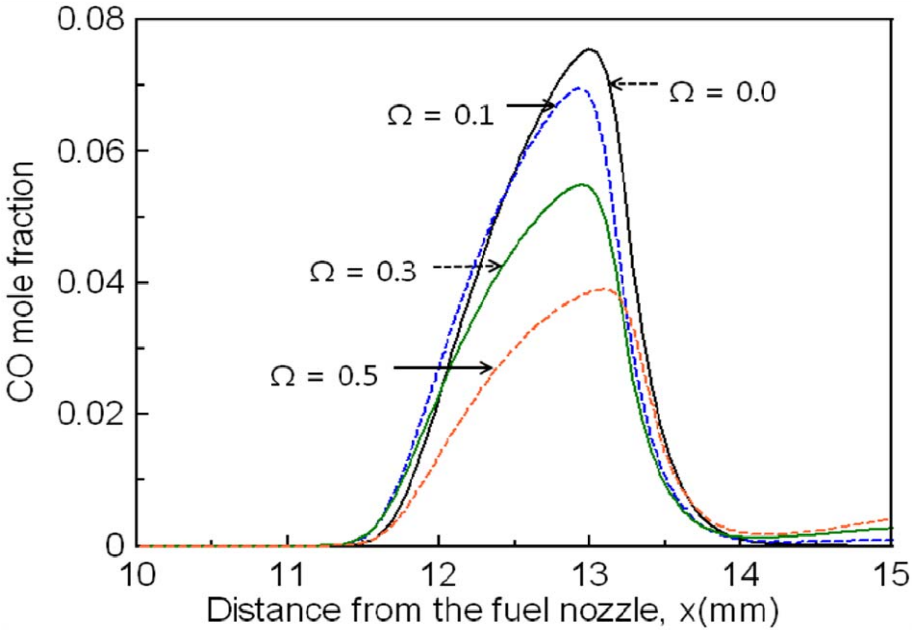

Figure 6. Distribution of CO mole fraction CH_4 nonpremixed flame ignited by hot air with the variation or dilution rate at a_g=1000 (1/s).

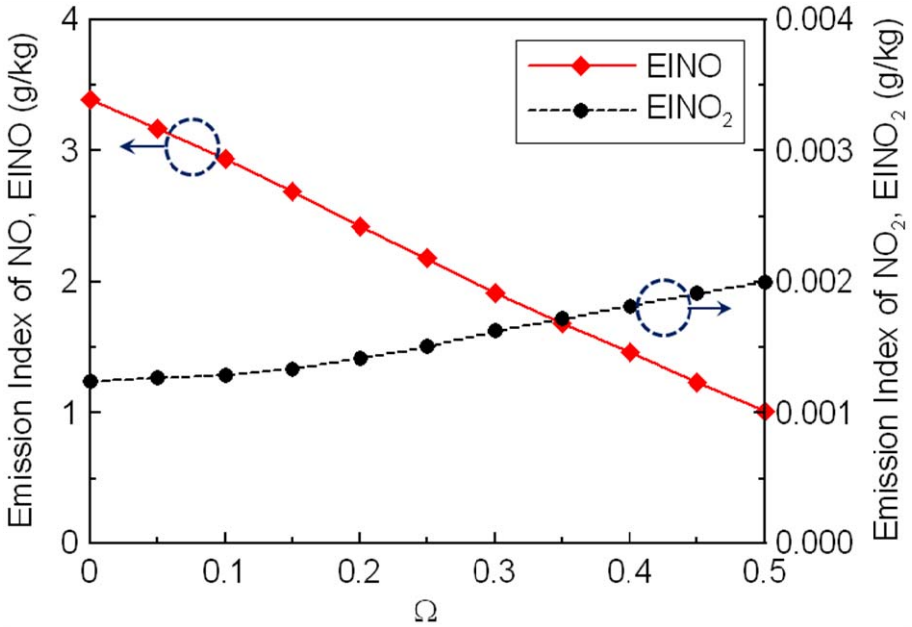

Figure 7. Variation of emission indices for NO and NO_2 with dilution rate at a_g=1000 (1/s).

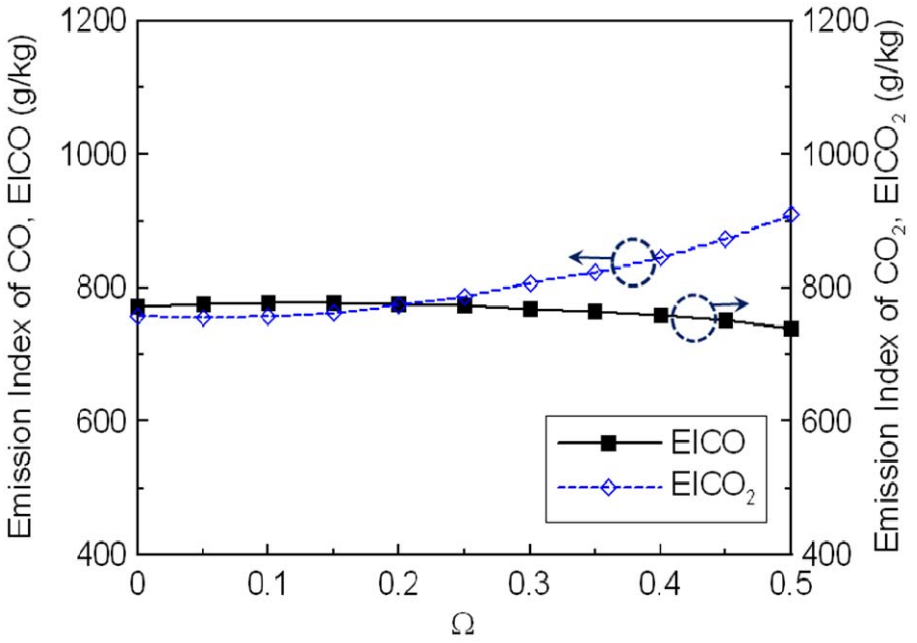

Figure 8. Variation of emission indices for CO with dilution rate at a_g=1000 (1/s).

Conclusions

Ignition of CH_4 by counterflowing hot air diluted with combustion products was investigated numerically to examine the combustion characteristics in the region between fresh fuel and diluted air with burnt gases of high-temperature air combustor. Flame structure and emission characteristics of CH_4 nonpremixed flame ignited by the diluted hot air were also investigated. The main results are as follows:

Ignition temperatures of CH_4 by hot air in the function of the global strain rate were obtained using a flame-controlling continuation method. The ignition temperature increases with the global strain rate for a fixed dilution rate. The ignition temperature also increased with the dilution rate for a fixed global strain rate. For large global strain rates, the increase rate of the ignition temperature further increased compared to the increase rate of dilution rate.

EINOx in F/BA region decreased remarkably with increasing the dilution rate for the fixed global strain rate. The EINOx for the condition considered in this study ($\Omega \leq 0.5$) was still higher than that of usual low-temperature air nonpremixed combustion or BF/A region. Furthermore, EICO decreased slightly but $EICO_2$ increased gradually with increasing the dilution rate. It was identified that the BF/A region of high-temperature air combustor contributes to the reduction of CO emission but is not effective in reducing the CO_2 emission even by increasing the dilution rate.

Acknowledgments

This research was supported by Basic Science Research Program through the National Research Foundation of Korea (NRF) funded by the Ministry of Education, Science and Technology (No. 20110004602).

Nomenclature

a_g	Global strain rate
Ω	Dilution rate

References

[1] Katsuki, M., Hasegawa, T., "The Science and Technology of Combustion in Highly Preheated Air", *Twenty-Seventh Symposium (International) on Combustion*, Boulder, Colorado, pp 3135-3146.

[2] Cavaliere, A., Joannon, M., "Mild Combustion", *Progress in Energy and Combustion Science* 30: 329-366 (2004).

[3] Maruta, K., Muso, K., Takeda, K., Niioka, T., "Reaction Zone Structure in Flameless Combustion", *Proceedings of the Combustion Institute* 28: 2117-2123 (2000).

[4] Mohamed, H., Benticha, H., Mohamed, S., "Numerical Modeling of the Effects of Fuel Dilution and Strain Rate on Reaction Zone Structure and NOx Formation in Flameless Combustion", *Combust. Sci. and Tech.* 181: 1078-1091 (2009).

[5] Jutz, A.E., Kee, R.J., Grcar, J.F., Rupley, F.M., "OPPDIF: A Fortran Program for Computing Opposed-Flow Diffusion Flames", *Sandia National Laboratories Report* SAND96-8243 (1997).

[6] Nishioka, M., Law, C.K., Takeno, T., "A Flame-Controlling Continuation Method for Generating S-Curve Responses with Detailed Chemistry", *Combustion and Flame* 104: 328-342 (1996).

[7] Oh, C.B., Lee, E.J., Jung, G.J., "Unsteady Auto-ignition of Hydrogen in a Perfectly Stirred Reactor with Oscillating Residence Times", *Chemical Engineering Science*, submitted (2011).

[8] Chelliah, H.K., Law, C.K., Ueda, T., Smooke, M.D., Williams, F.A., "An Experimental and Theoretical Investigation of the Dilution, Pressure and Flow-Field Effects on the Extinction Condition of Methane-Air-Nitrogen Diffusion Flames", *Proceedings of the Combustion Institute* 23: 503-511 (1990).

[9] Takeno, T., Nishioka, M., "Species Conservation and Emission Indices for Flames Described by Similarity Solutions", *Combustion and Flame* 92: 465-468 (1993).

[10] Sung, C.J., Law, C.K., Chen, J.Y., "Augmented Reduced Mechanisms for NO Emission in Methane Oxidation", *Combustion and Flame* 125: 906-919 (2001).

[11] Song, K.M., Oh, C.B., "A Study of the Ignition Characteristics of CH_4-hot Air Diffusion Flame using a Flame-Controlling Continuation Method", *41th Korean Society of Combustion Symposium*, Kyeonggi, Korea, pp 7-14.

[12] Egolfopoulos, F.N., Dimotakis, P.E., "Non-premixed Hydrocarbon Ignition at High Strain Rate", *Twenty-Seventh Symposium (International) on Combustion*, Boulder, Colorado, pp 641-648.

[13] Liu, W., Lu, T., Law, C.K., "The Role of Double-turning in Counterflow Ignition of Methane, Ethylene and Methane/Hydrogen Mixtures", *46th AIAA Aerospace Sciences Meeting and Exhibit*, Reno, Nevada, pp 994-1005.

[14] Fotache, C.G., Sung, C.J., Sun, C.J., Law, C.K., "Mild Oxidation Regimes and Multiple Criticality in Nonpremixed Hydrogen-Air Counterflow", *Combustion and Flame* 112: 457-471 (1998).

[15] Kreutz, T.G., Law, C.K., "Ignition in Nonpremixed Counterflowing Hydrogen versus Heated Air: Computational Study with Detailed Chemistry", *Combustion and Flame* 104: 157-175 (1996).

[16] Fotache, C.G., Kreutz, T.G., Law, C.K., "Ignition of Hydrogen-Enriched Methane by Heated Air", *Combustion and Flame* 110: 429-440 (1997).

[17] Blouch, J.D., Law, C.K., "Non-premixed Ignition of n-heptane and iso-octane in a Laminar Counterflow", *Proceeding of the Combustion Institute* 28: 1679-1686 (2000).